CHAPTER SIX

The effect of icing events on the death and regeneration of North American trees

Charles A. Nock[a], Kathleen F. Jones[b], and David F. Greene[c]
[a]Department of Renewable Resources, University of Alberta, Edmonton, AB, Canada
[b]Cold Regions Research & Engineering Laboratory, US Army Corps of Engineers, Hanover, NH, United States
[c]Department of Forestry and Wildland Resources, Humboldt State University, Arcata, CA, United States

Introduction

Literature dating back to the early 20th century reveals a long-standing interest, almost entirely by foresters in eastern North America, on the effect of ice deposited on trees (Abell, 1934; Whitney and Johnson, 1984; Bruederle and Stearns, 1985; Belanger et al., 1996). Although ice events also occur in the boreal forest and west of the prairies, little has been written about the effect of freezing precipitation on forests in this area. The map in Chapter 5, fig. 5.6, showing the annual average number of hours of freezing rain, provides only limited information on the probability of damaging freezing rain (and drizzle) storms. The term "freezing precipitation" refers to both freezing rain and freezing drizzle, with drop diameters of about 1 and 0.1 mm, respectively. As shown by the maps of icing severity for a 500-year mean recurrence interval in reports by the Canadian Standards Association (CSA, 2001), Jones et al. (2002), and the American Society of Civil Engineers (ASCE, 2017), freezing precipitation storms are particularly severe in a swath extending northeasterly from Oklahoma, Arkansas, and Missouri, across southwest Ontario and adjacent portions of the northeastern states, and into the Atlantic provinces of Canada. South, west, and north of this belt, freezing precipitation events tend to be less severe, but storms that damage trees and power lines occur even in Texas and the southeastern states and are relatively frequent in the Piedmont of the Carolinas. In the northwestern United States, freezing precipitation tends to occur with high winds in the Columbia River Gorge, and significant events with lower wind speeds occur in the Willamette Valley of Oregon and the Fraser Valley area in

https://doi.org/10.1016/B978-0-12-818813-2.00006-X

Washington and British Columbia. Elsewhere west of the Rockies, damaging freezing precipitation storms are quite rare.

Early studies of ice events (Von Schrenk, 1900; Harshberger, 1904; Illick, 1916; Rhoades, 1918; Rogers, 1922, 1923, 1924) were descriptive, often simply documenting an event that had occurred and the approximate area of forest that had been affected. The more recent literature (Cannell and Morgan, 1989; Nicholas and Zedaker, 1989; Seischab et al., 1993; Jones et al., 2001; Proulx and Greene, 2001; Rhoads et al., 2002; Yorks and Adams, 2003) adopts a much more analytical approach to freezing precipitation events and forest damage. The most recent developments in the field have included novel analytical approaches combined with simulated icing (Rustad and Campbell, 2012; Nock et al., 2013, 2016; Fahey et al., 2020). While research interests and methods vary widely, studies have centered on species-specific responses (based on post event damage assessments) and have often been presented as ordinal scale comparisons of species' susceptibility to damage (e.g., low, moderate, and high, or some similar system) (Abell, 1934; Downs, 1938; Kienholz, 1941; Carvell et al., 1957; Lemon, 1961; Goebel and Deitschman, 1967; Whitney and Johnson, 1984; Bruederle and Stearns, 1985; Boerner et al., 1988; Hauer et al., 1993; Rebertus et al., 1997). This more recent literature often leaves the impression that *everything* matters: accumulated ice thickness, wind velocity, topography, tree size (bole diameter and major branch diameter and length) and species' "intrinsic" resistance to injury, exemplified by attributes such as branching architecture and wood density, and has led to little agreement on species-specific or size-specific susceptibility. A process-oriented approach could not merely provide useful data sets but, more important, unambiguously specify what *should* be measured in future investigations.

There has been another major problem in almost all of these studies; aside from icing events in urban settings, it is difficult—but, as we will argue below, not impossible—to measure ice accretion in a stand because: (1) the ice is often melting within 24 h of the damage; (2) some roads are closed during the period that the ice remains on branches; and (3) we normally cannot extrapolate from ice thickness measurements elsewhere because icing severity varies significantly within the affected region and there may well be no ice or much more ice at the nearest reporting station. Thus, few studies of damage to trees have estimated ice thickness. Further, in post hoc, interspecific comparisons within a single study, it is implicitly assumed that ambient ice thickness was similar for all species. But this may not be true when many transects are used, especially in the mountains, where small differences

in altitude can lead to great differences in ice thickness and, of course, species tend to be arrayed along contours.

The climatology and meteorology of icing events were reviewed in Chapter 5. Individual ice events vary considerably in terms of the type of icing that occurs, as well as the intensity (ice thickness), persistence, and wind speeds during the disturbance. In addition to snow storms, the two types of icing with the greatest potential for bole or branch damage are glaze ice and rime ice. Glaze ice is usually clear, smooth, and hard; contains some air bubbles; and has a density of approximately $900\,\mathrm{kg\,m^{-3}}$. Rime ice is opaque, with individually frozen cloud or fog droplets separated by pockets of air and, therefore, of a density about 30–90% that of glaze ice. Hoarfrost, a low-adhesion, feathery deposit of ice crystals formed from water vapor, may also build up on surfaces but is unlikely to cause branch damage because the total added mass is quite small (McKay and Thompson, 1969). We discuss damage associated with glaze ice from freezing precipitation storms.

Meanwhile, the consequences of major icing episodes for stand competitive dynamics will depend greatly on how often such events recur (Fig. 6.1). The measure of interest is the mean recurrence interval, which is defined as the inverse of the annual occurrence rate. For example, an ice thickness with a 50 year mean recurrence interval has a 1/50 or 0.02 probability of being exceeded in any year, and a probability of 0.33 of being exceeded in any 20-year period. These measures for mean recurrence interval have often been reported informally as *regional* mean recurrence interval for major events. Thus, we have a report of a mean recurrence interval of 20–100 years for

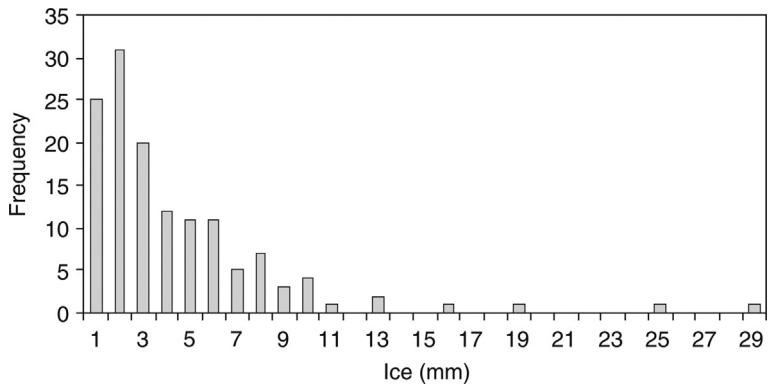

Fig. 6.1 Ice thickness (added cylinder diameter $= 2t_{max}$) at St. Faustin (Quebec, Canada) and measured on horizontal wooden 25 cm dowels for the period 1977–1997. The aggregated dataset includes icing from 136 events. *(Data courtesy of Hydro-Québec).*

"major" storms of unspecified intensity in northern hardwood forests of eastern North America (Melancon and Lechowicz, 1987) and approximately 20 years for northern Missouri forests (Rebertus et al., 1997). A regional mean recurrence interval is not useful for understanding the risk posed by recurrent icing events of specific magnitude for a randomly chosen tree. These foregoing quantifications cannot even suggest that icing disturbance in a particular region is more or less recurrent, at a point, than other forest disturbances, such as stand-replacement fires (Lorimer and Frelich, 1994) or perhaps catastrophic blowdowns (Lorimer, 1977; Canham and Loucks, 1984; Frelich and Lorimer, 1991). There are, however, point estimates for ice thickness for Canada (CSA, 2001) and the United States (ASCE, 2017) for use in the design of ice-sensitive structures, including power transmission lines and tall towers. These maps, showing equivalent radial ice thickness with concurrent gust speeds for a 50 year mean recurrence interval (with factors for adjusting the mapped values to other mean recurrence interval), have not been used in the ecological literature until now.

Our primary objective in this chapter is to introduce a biomechanical interpretation of branch breakage as a function of ice thickness, wind speed, and branch length. The exercise is perhaps too simple, but it will serve to express the interaction of these three fundamental factors. We then discuss other factors that affect the likelihood that any given branch in a forest canopy will break in an ice storm. We follow with a review of the empirical literature on tree damage due to ice, and finally, discuss recent experimental approaches to understanding icing impacts on forests that employ simulated icing.

The biomechanics of branch breakage during ice events with and without wind

Ice accretion on branches

As discussed in Chapter 5, freezing rain occurs when a warm air mass with a temperature aloft greater than 0 °C slides above a colder air mass with a ground-level temperature below freezing. A snowflake is formed above the warm air layer, melting as it falls through the warm air and becoming supercooled during the descent through the cold air layer at the surface. Eventually it may strike a horizontal surface (flat roof, sidewalk, horizontal branch) that has had time to adjust to the freezing temperatures of the cold air mass. Assuming that it is cold and windy enough that the intercepted

drops freeze and if the precipitation is not intercepted by nearby taller elements, the thickness of the ice, t_s (m), on a horizontal surface, is

$$t_s = 1.1 t_p \tag{6.1}$$

where t_p is the depth (m) of the accumulated water and 1.1 is the ratio of the density of water to glaze ice.

The literature on the icing of cables, towers, and other structures uses the *equivalent radial ice thickness* (t) as the standard measure of ice accretion in freezing rain. This is the radius of ice added to the cylinder radius that would occur if the ice were distributed uniformly around the cylinder circumference. Jones (1998) developed a simple model (hereafter Simple model) for the equivalent radial thickness of ice accumulating on a horizontal cylinder, oriented with its axis perpendicular to the wind direction, intercepting rain or drizzle drops. We note that, due to a number of simplifying assumptions, the Simple model overestimates ice loads relative to recently published icing models (details in Sanders and Barjenbruch, 2016). Assume that the ice freezes uniformly thickly around the cylinder, which might occur when the branch or wire or cable twists in response to an asymmetric accretion (because of wind-blown precipitation or when the impinging water flows on the surface briefly before freezing). Then, in the absence of wind, the equivalent radial ice thickness is

$$t = t_s/\pi = 0.35 t_p \tag{6.2}$$

Note that this radius of ice is independent of the original cylinder diameter, and thus we expect the ratio of ice thickness to branch diameter to be very large near the branch tip but much more reduced axially. By adding the effect of wind to this idealized accretion process, and simplifying the relationship between the precipitation rate and the liquid water content of the air, then

$$t = (t_s/\pi)\left[1 + (\overline{u}/5)^2\right]^{0.5} = 0.35 t_p \left[1 + (\overline{u}/5)^2\right]^{0.5} \tag{6.3}$$

where $\overline{u}$ is the local mean wind speed in $\mathrm{m\,s^{-1}}$ during freezing rain. This is the "back-of-the-envelope" version of the Simple model of Jones (1998), in which the factor 5 is the fall speed of the rain drops in $\mathrm{m\,s^{-1}}$. The complete Simple model uses the time-varying precipitation rate and wind speed, and the fall speed of the drops is a function of the precipitation rate. The added ice mass $m_i(x)$ per unit length at x along the branch (i.e., the added area multiplied by the density of ice, ρ_i) is

$$m_i(x) = \rho_i \pi \left(t^2 + d(x)t\right) \tag{6.4}$$

where $d(x)$ is the wood diameter at distance x distal from the branch tip. The ratio of ice mass to wood mass (assuming $800\,\mathrm{kg\,m^{-3}}$ for wood density) is shown as a function of branch diameter in Fig. 6.2. For this figure, the assumed wind speed is $5\,\mathrm{m\,s^{-1}}$, and the total ice thickness on a horizontal surface, t_s, is 0.09 m (9 cm, an extremely large value), giving a radial ice thickness from Eq. (6.3) of 0.04 m (a bit less than the maximum reported during the 1998 event discussed in Chapter 5). Near the branch tip at a diameter of 0.002 m, the ice/wood mass ratio is about 1900, while near the base of a 3-m-long branch at a branch diameter of 0.053 m, the ratio is about 6. Thus, the lack of dependence of the radial ice thickness on diameter leads to a much greater relative increase in the vertical load at the branch tip than at the base. However, the mass of ice per unit length (Eq. 6.4) near the tip of the branch is smaller than near the base, $4.9\,\mathrm{kg\,m^{-1}}$ compared to $10.7\,\mathrm{kg\,m^{-1}}$. Note that the independence of radial ice thickness and diameter is not unique to this Simple model; in other ice accretion models for freezing rain in which the accreted ice thickness is allowed to vary with the branch diameter and a heat balance calculation is used to determine the fraction of the impinging water that freezes, it still remains essentially constant (Jones, 1998).

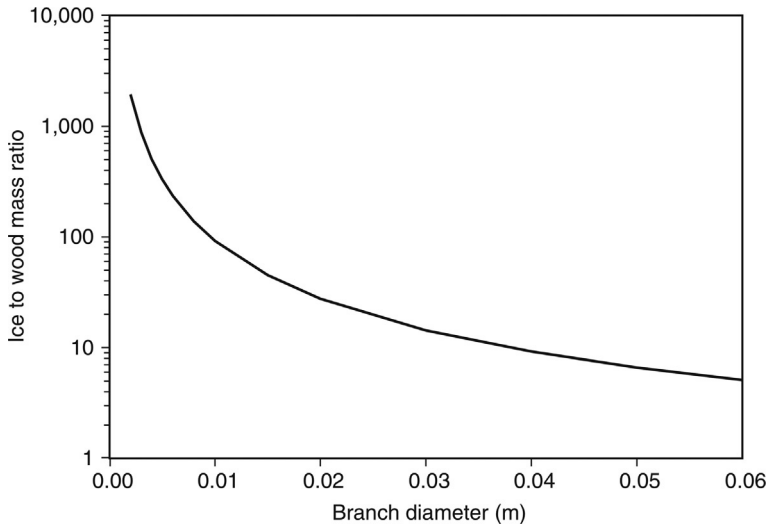

Fig. 6.2 The ratio of ice mass to wood mass as a function of position (diameter) on a branch for an equivalent radial ice thickness (t) of 0.04 m.

Now we need to embed this accretion model into the calculation of the stress on a branch. The accumulated ice can increase the resultant force on a branch element in two ways. First, the added area increases the drag exerted by the wind and second, the added mass increases the weight on the branch. We deal first with the drag.

Effect of wind on the ice-laden branch

The wind's drag force per unit length $D(x)$ on the shoot element at distance x distal from the branch tip is

$$D(x) = (\rho_a/2)\, d(x)\, u^2 C_D \tag{6.5}$$

where ρ_a is the density of air ($1.2\,\mathrm{kg\,m^{-3}}$), u is the ambient wind speed ($\mathrm{m\,s^{-1}}$) near the element of interest (typically increasing with height above ground), $d(x)$ is the diameter at x (m), and C_D is the drag coefficient (which we can assume to be 1.0 at the Reynolds numbers of interest).

What wind speeds might be expected while the branches are ice-covered? Imagine a 25 m tall hardwood forest with all the branches located in the upper 50% of the forest and with crown midpoints located at 18.75 m. In *open* areas, the expected 3 s gust speed following major icing events while the air temperature remains below freezing and the accumulated ice remains on branches is $20\,\mathrm{m\,s^{-1}}$ in much of the United States (ASCE, 2017). Speeds are lower in the southern states, where the air tends to warm more quickly after freezing precipitation ends (so there is less opportunity for very strong winds to occur concurrently with ice-covered branches) and higher in the north-central states, where winters tend to be cold. How strong will the winds be within an adjacent forest near the open area where measurements were made? There will, of course, be a steep gradient in the wind speed profile just above and within the crown space (Greene and Johnson, 1996). Assuming a $20\,\mathrm{m\,s^{-1}}$, 3 s gust at 10 m in the open, we can estimate the *fastest speed* at 18.75 m in a *leafless* forest using the protocol of Greene and Johnson (1996)—$u_c = 0.47\ u_{r10}$ where u_{r10} is the reference speed at 10 m height in an open area and u_c is the horizontal speed midway in the crown. Thus, the gust speed expected to occur at the midcrown height while ice remains on the branches following a major storm is about $10\,\mathrm{m\,s^{-1}}$.

There is a further consideration regarding the relationship between branch length and wind speed: given ramification, longer branches tend to be located lower within the crown and therefore experience slower wind speeds than branches higher in the crown. This complexity is ignored in the

following calculations, and a constant wind speed is assumed over the length of the branch.

We initially idealize a branch as a cantilever lacking both side shoots and leaves with diameter increasing basally from the branch tip toward the bole. We need to allometrically relate distance from the branch tip (x) to the diameter ($d(x)$) at that point. Niklas (2000) has calculated the relationship for the eastern hardwood species *Prunus serotina* Ehrh. (black cherry) as:

$$\log x = 1.16 + 0.166 \log d(x) - 0.29 \left(\log d(x)\right)^2 \tag{6.6}$$

where the logarithm is base 10. (Note that Niklas (2000) erroneously writes 1.66 rather than 0.166 (as above) in both his figure caption and in his text.) In what follows we will use the allometry of this cherry as typical of eastern hardwoods. For branches up to 3 m long, Eq. (6.6) is fit very well by the linear relationship

$$x = ad(x) + b \tag{6.6a}$$

where $a = 59.26$ and $b = -0.0956$ m. This linear form will be used in calculating the stress at the base of the branch.

The bending moment M (defined as a force multiplied by a length) on the entire branch is the integral of the moments from the elemental sections dx from the tip to the base:

$$M = \int_0^{x_T} \frac{1}{2} C_D p_a u^2 [d(x) + 2t](x_T - x)dx \tag{6.7}$$

where x_T is the total length of the branch. Using the linear variation of the diameter of the branch along its length results in

$$M = \frac{1}{2} C_D p_a u^2 x_T^2 \left(\frac{x_T}{6a} - \frac{b}{2a} + t\right) \tag{6.7a}$$

Finally, the bending stress (a force per area: a pressure), s, at the branch base is given by

$$\sigma = Md_T/(2I) \tag{6.8}$$

where $d_T = (x_T - b)/a$ is the basal diameter and I is the moment of inertia ($I = p(d_T/2)^4 4$). The stress at which the branch breaks (the breaking stress) can be found in published compendia for "green" wood specimens (recently cut and containing moisture). These values range from about 30 to 90 MN m^{-2} for North American trees; hence we will use 60 MN m^{-2} as

a typical breaking stress in the following calculations. We note that any prior damage to a branch acts as a stress rise, so a branch with a cavity, a canker, or any other sort of defect or damage will fail at a stress lower than the nominal breaking stress for that kind of tree (Kane et al., 2001).

The result of this calculation of ice-augmented drag on a 3 m long branch is shown in Fig. 6.3 for the range of radial ice thicknesses (0.01–0.05 m) that encompasses the deposition experienced from north to south across southern Quebec during the 1998 icing event. Given the dependence of drag on the square of the wind speed, it is not surprising that the bending stress is more sensitive to wind speed than to ice thickness, which is a linear term in Eq. (6.7a).

The effect of branch length on the bending stress is shown in Fig. 6.4 for a wind speed of $10\,m\,s^{-1}$ for non-foliated branches and across the range of radial ice thicknesses of interest. The stress peaks at a branch length of about 0.2 m. The magnitude and location of the peak are determined by the

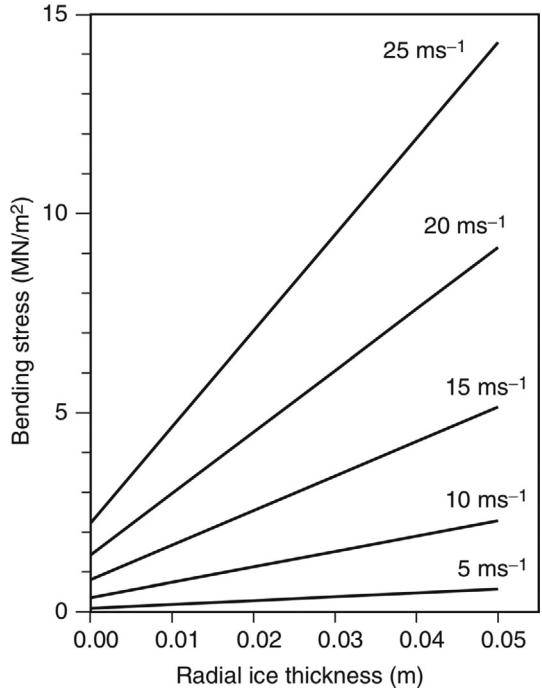

Fig. 6.3 The effect of wind-induced drag: stress vs equivalent radial ice thickness (*t*) where there has been no interception by higher branch elements for a 3 m long horizontal branch. u denotes the ambient wind speed ($m\,s^{-1}$).

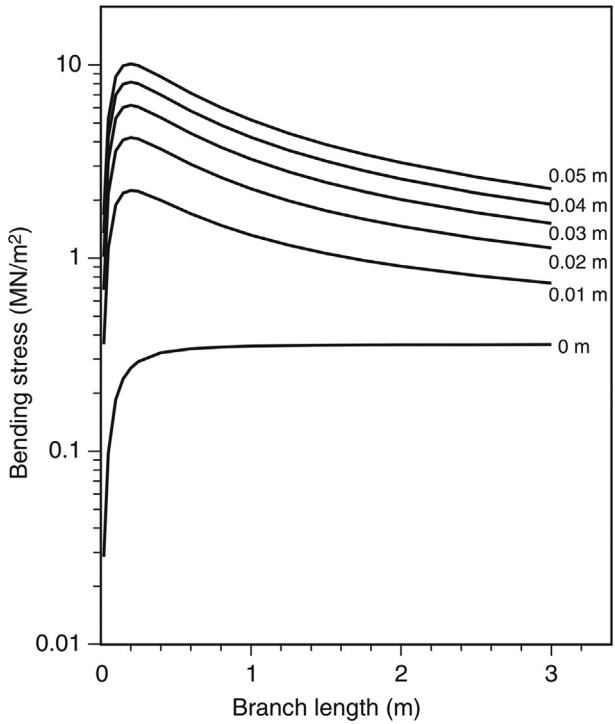

Fig. 6.4 The effect of wind drag: stress as a function of branch length for equivalent radial ice thicknesses from 0 to 0.05 m with an ambient wind speed of 10 m s^{-1}.

parameters a and b (Eq. 6.6a), where b/a is the minimum branch diameter (1.6 mm). If b is doubled, the peak stress decreases by about 50% and occurs at a branch length of 0.4 m. If the rate of increase of branch diameter with length (the parameter a) is greater than in Eq. (6.6a), the peak stress increases, but the peak still occurs at a branch length of 0.2 m. At a wind speed of 10 m s^{-1}, the stress from wind drag on this nonramified cantilever is significantly less than the breaking stress, even at the peak.

We should perhaps not take too seriously the mode in Fig. 6.4 because this calculation has ignored the probably much less compact shape of the actual ice accretion and has not included shoot ramification; the ice-enhanced drag will be greater for entire branch units than pictured here, and the bias is especially great for longer branches, which will have more side shoots than shorter branches. This added complexity is discussed in more detail later in this chapter.

Effect of gravity on the ice-laden branch

Of course, the additional weight of the ice applies a significant load to the branch, whether or not the wind is blowing. The drag in Eq. (6.7) is replaced by the weight (total mass multiplied by the gravitational acceleration), and so the bending moment M_g is

$$M_g = \int_0^{xT} \pi p_i g \left[d(x)t + t^2 \right] (x_T - x) dx \tag{6.9}$$

where g is the gravitational acceleration ($9.8\,\mathrm{m\,s^{-2}}$). This equation uses the ice mass per unit length from Eq. (6.4). The bending stress is, as in Eq. (6.8), equal to $Md_T/(2I)$ and the diameter variation is given by Eq. (6.6a). Integrating Eq. (6.9) gives

$$M_g = 0.5 p_i g x_T^2 t \left(\frac{x_T}{3a} - \frac{b}{a} + \mathrm{t} \right) \tag{6.9a}$$

The bending stress from the ice weight is plotted in Fig. 6.5. In the absence of ice ($t_s = 0$), the stress rises with branch length but is, as one would expect, far below the breaking stress for healthy branches.

As for wind drag, the situation is quite different as ice is added; stress peaks at a branch length of about 0.2 m, and the location and magnitude of the peak depend, as with wind drag, on the minimum branch diameter and the rate of increase of diameter with distance from the tip. Interestingly, the stress from branch weight, both with and without ice, is much greater than that from the wind drag; an icing event with a radial ice thickness greater than 0.04 m should cause the loss of branches less than 0.5 m long even in the absence of wind. By contrast, the $10\,\mathrm{m\,s^{-1}}$ gust speeds at midcanopy height that are expected after an icing event could not break healthy branches if wind drag were the only stress. The effects of ramification on gravity-induced stress are examined in the following section.

Complications

This modeling is an initial foray; much that could make it more realistic and applicable to individual trees or forest stands is still missing. In this section we discuss: (1) branch ramification, (2) bole snapping from wind drag on an entire tree, (3) branch deflection and orientation, (4) ice persistence, (5) canopy position, and (6) breaking strength.

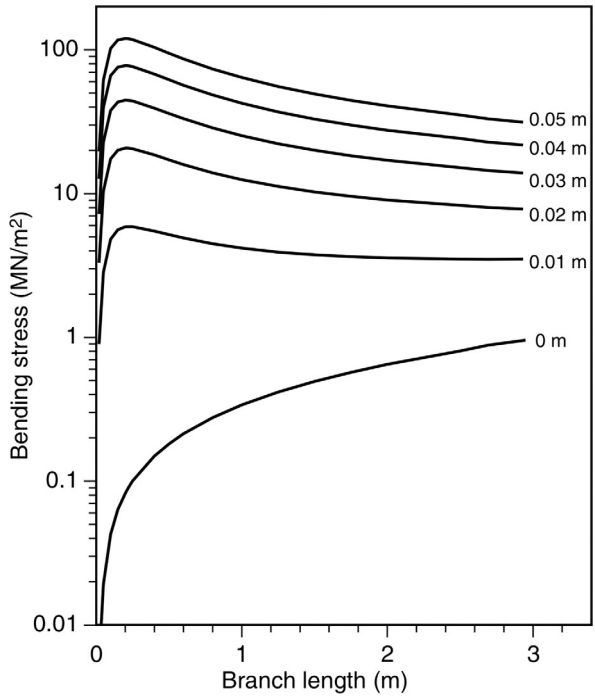

Fig. 6.5 The effect of gravity: stress as a function of branch length for equivalent radial ice thicknesses from 0 to 0.05 m.

Individual branches need to be treated more realistically as a ramified set of shoots possessing a varied set of branching angles and, in the case of non-*Larix* conifers, leaves attached. (Occasionally of course, icing events occur when hardwoods or *Larix* still have leaves attached, particularly in regions where cold winters are not the norm.) To examine the effect of ramification on ice-augmented stresses from both wind and gravity, we cut a healthy, 2.76 m long black cherry branch from a 15 m tall tree at Mt. St. Hilaire, Quebec. Ignoring leaves, we measured the length and branching point of every shoot, working outward apically from the base. The total length of these side shoots was 30.7 m, increasing the length of the entire unit by an order of magnitude. The actual branch geometry was then idealized to simplify the calculation of moments and to examine the effects of branching angle and length of side shoots. All shoots arising from the main branch were assumed to be at the same constant angle to the main branch, and each subshoot was assumed to be parallel to these main shoots. The bending stress at the base of the ramified branch (as well as that of the simple cantilever we

assumed earlier in this chapter) is shown in Fig. 6.6A (wind drag) and Fig. 6.6B (gravity) for angles of 90° (main shoots horizontal and perpendicular to the main branch), 45°, and 0° (main shoots pointing in the same direction as the main branch). Also shown is the bending stress for a pruned branch, with all except the side shoots arising directly from the main branch removed—this pruning reduces the total length of shoots from 30.7 to 10.6 m.

For our expected $10\,m\,s^{-1}$ maximum gust at midcanopy, the wind load on this branch unit still does not cause a bending stress exceeding the average breaking stress of $60\,MN\,m^{-2}$, even for a 0.05 m radial ice thickness. However, the addition of side shoots also increases the bending stress from the gravity load so that this ramified branch could be broken by the $10\,m\,s^{-1}$ gust if the radial ice thickness exceeded 0.015 m. This threshold ice thickness is roughly correct for the ramified branch for all assumed branching architectures. The removal of the higher-order shoots reduces the bending stress from either wind load or gravity load by about 60% for this range of ice thicknesses. For this pruned branch, the required radial ice thickness to cause failure at a gust speed of $10\,m\,s^{-1}$ doubles to about 0.03 m. While these calculations ignore the real variations in branching architecture that occur, they show that the ice on side shoots in a branch unit contributes significantly to the bending stress at the base of the branch, and that the total length of the side shoots is more important than the branching architecture. Note that these results are for this particular 2.76 m branch unit and provide only

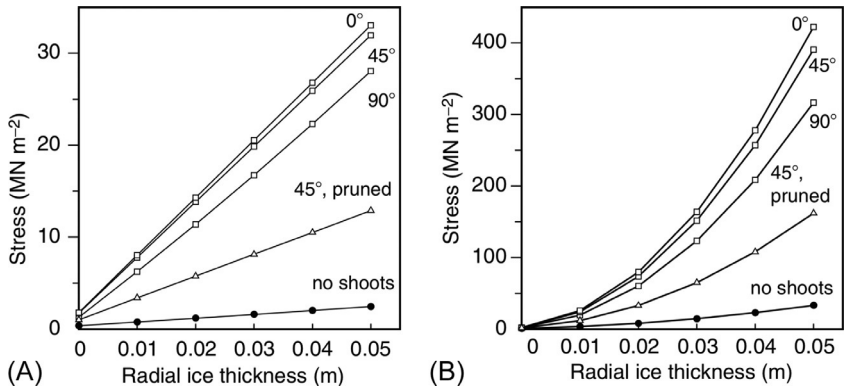

Fig. 6.6 Bending stress on a ramified 2.76 m branch compared to a branch with no side shoots, showing the variation of stress with branching architecture and pruning. (A) Wind load (with an ambient speed of $10\,m\,s^{-1}$ and (B) gravity load.

one example of the increase in bending stress that might be expected for a ramified branch compared to a nonramified branch.

The augmentation of the wind-induced bending moment due to ice on an entire tree (i.e., bole snapping) is worth examining as well. A rough calculation can be done by using the 8.5 m tall ash (*Fraxinus*) in Jones (1999). If we assume that the 1538 m of total branch length on the ash are uniformly distributed over the canopy from 3 to 8.5 m, then the moment from the wind drag on the tree can be estimated from $L(d)$, which is the cumulative distribution of branch length with diameter less than d

$$L(d) = L_T e^{-(d_0/d)^2} \tag{6.10}$$

where the total branch length is $L_T = 1538$ m and a characteristic branch diameter is $d_0 = 0.0041$ m for this tree. For this cumulative distribution, the median branch diameter (half of the total branch length has a larger diameter) is $-d_0/\ln(0.5^{1/2}) = 0.012$ m. At the base of the stem, the bending stress (s_{tree}) is

$$\sigma_{tree} = 0.5 C_D \rho_a u^2 H L_T \left(2t + d_0\sqrt{\pi}\right) / \left(0.25\pi (d_{tree}/2)^3\right) \tag{6.11}$$

where $H = 5.75$ m is the distance from the base of the stem, with diameter $d_{tree} = 0.28$ m, to the midcanopy height. For this tree, the value of $d_0\sqrt{\pi}$ is 0.007 m, so a radial ice thickness of only 0.01 m would more than triple the bending stress in the stem from the wind drag. A radial ice thickness of 0.03 m increases the bending stress by an order of magnitude. Note that these increases in stress are similar in magnitude to what we calculated for 1 m long unramified branches (Fig. 6.4). The moment in the stem is high compared to the moment in either the unramified branches in Fig. 6.4 or the ramified cherry branch in Fig. 6.6A because the wind is acting on all 1538 m of branches. However, because of the large stem diameter compared to the branch diameter, the stress in the stem exceeds the breaking stress only at high wind speeds. With no ice, the bending stress at the base of the stem exceeds the average breaking stress at a wind speed of 58 m s^{-1}. At radial ice thicknesses of 0.01 and 0.03 m, the wind speed necessary to exceed this breaking stress is reduced to 30 and 19 m s^{-1}, respectively.

We have ignored the branch deflection due to the ice loading and the wind drag, which will decrease the stress at the base of the branch (Bisshopp and Drucker, 1945; Leister and Kemper, 1973). Another factor—not dealt with here—is the relative orientation of the branch to the wind direction and to the vertical. For simplicity, we have assumed a

horizontal branch oriented perpendicular to the wind. But of course branches with orientations oblique to the wind and to gravity will be the norm; wind and ice loads on those branches will be smaller than shown here. At the extreme, the wind load on a branch parallel to the wind direction will be from skin friction only, which is very small compared to the form drag, and the additional bending load due to ice on a branch (or, more cogently, a bole) that is close to vertical will be almost zero. However, the orientation of the branch may change in the course of an ice storm as the branch unit or tree sags, bends, or leans, changing the wind and gravity environment of individual branches. This latter point reemphasizes the preliminary nature of our modeling effort.

As mentioned earlier, the concurrent gust speeds in the ASCE map of 500 year ice thicknesses generally increase from regions that tend not to have cold winters to regions where long cold winters are the norm, reflecting the expected increase in persistence of the accreted ice. This regional map does not show, however, local areas where temperatures remain cold longer than in the surrounding region perhaps because of higher terrain; nor does it show local areas where wind speeds tend to be higher than at the airport weather stations. A serious analysis of ice-induced damage in a particular region will need to deal with the local residency period; that is, how long the accumulated ice remains on the trees. Clearly, the chance of wind-related tree damage increases with the length of time the ice persists (Elfashny et al., 1996; Jones et al., 2002). Often, ice accretion is followed by above-freezing temperatures as the cold air layer at the surface is eroded away by the advancing warm air mass, but ice can remain long after an icing event (Schaub, 1996). In Quebec, Elfashny et al. (1996) reported that ice residence time for most events was limited to between 1 and 2 days. Nonetheless, at a few stations in Quebec, especially at high latitudes, residency periods over a month long have been recorded. As pointed out in Chapter 5, the 1998 event that devastated the forests of southeastern Canada and the northeastern United States was unusual because it included two periods of precipitation over a 5-day period with the initially accreted ice not melted before precipitation was renewed.

We have ignored the dependence of ice accretion on canopy position, using the expected gust speed at midcanopy in calculating the bending stress from the wind load. However, less ice is expected to accrete on lower branches and more on branches near the top of the canopy, both because higher branches in the canopy intercept some of the precipitation and because wind speeds decrease from the top to the bottom of the canopy. For the typical

$5\,m\,s^{-1}$ wind speeds in open areas during freezing rain storms, the ice thickness gradient in the canopy is small because of the low wind speeds, ranging from $3.8\,m\,s^{-1}$ at the top of the canopy to $1.4\,m\,s^{-1}$ at the bottom. Using this wind gradient from Greene and Johnson (1996) results in radial ice thicknesses for $t_p = 0.03\,m$ varying from 0.011 to 0.013 m from the bottom to the top of the canopy. However, the prior interception of precipitation by the upper canopy will steepen this gradient. The median interception fractions for deciduous and coniferous forests for liquid precipitation are 13% and 22%, respectively (Dunne and Leopold, 1978). The interception fraction tends to be higher in light-precipitation (the norm for freezing precipitation events) than in heavy-precipitation events, and tends to be lower in the dormant season than in the growing season in deciduous forests. During freezing precipitation, the interception fraction will be greater than suggested by rain studies because of the near-zero stemflow and throughfall by leaf drip as the intercepted water freezes to the branches. Assuming 20% interception with the wind speed and precipitation depth given above, the ice thickness at the base of the canopy is decreased to 0.009 m. The positive feedback of the accreting ice causing the canopy to become denser preferentially near the top will further increase the vertical gradient in ice thickness over the course of the storm. This is compounded by the expected vertical variation in gust speeds following the freezing precipitation event. The $10\,m\,s^{-1}$ gust speed at midcanopy is consistent with winds of $15\,m\,s^{-1}$ at the top of the canopy and $6\,m\,s^{-1}$ at the bottom of the canopy. Thus, we expect greater stresses from both ice and wind for branches that are higher in the canopy.

Finally, we have ignored the variation in breaking stress of wood among different tree species, in the same species grown in different climates, and in different parts of the stem and canopy of an individual tree (Kane et al., 2001). For branches with a low breaking stress of $30\,MN\,m^{-2}$, Fig. 6.5 shows that unramified branches less than about 0.8 m long would break with a radial ice thickness of 0.03 m, while an ice thickness of over 0.05 m would be required to break a branch in that same length range with a breaking stress as high as $90\,MN\,m^{-2}$.

Predictions based on this biomechanical exercise

Our first prediction from the foregoing modeling is that, assuming there is enough ice to make the event worth categorizing as a serious icing phenomenon, the stress due to ice is far more important than that due to wind.

Nonetheless, the drag of the wind can be the hair that broke the camel's back. Toward the end of the 1998 event in the wooded area on Mount Royal in Montreal before the ice began to melt, one of us (Greene) noted qualitatively, yet unambiguously, that gusts of wind (during a day with very average wind speeds according to measurements at the nearby airport) were immediately followed by the "popping" sound of branches breaking and then the crash of the branches as they hit the ice-covered ground. One almost never heard branches breaking when there was no local gust simultaneously felt on one's face. There was no precipitation at the time of these observations; presumably, those branches sufficiently loaded with ice to break in relatively calm air had already fallen earlier in the week.

Oddly, the only quantitative information indicating that the wind matters in the amount of breakage during an icing event is that a few reports show that trees snapped and bent in the direction of the prevailing wind (with the prevailing wind taken from the nearest reporting station). Proulx and Greene (2001) found that the orientation of damaged stems was the same as that of the local wind on flat ground during the 1998 event in southern Quebec. This observation is similar to that of Nicholas and Zedaker (1989), who studied two severe icing events where the observed maximum icing diameter (*not* radial ice thickness) ranged from 0.07 to 0.10 m: they reported that generally, within a stand, tree stems and crowns were all snapped in a similar direction. We can imagine, then, that as ice accumulates on a branch, there comes a point where it can be broken by a small gust before it can be broken by the slower process of additional ice accretion. Thus, branches will lie on the ground primarily in the direction of the prevailing wind, and can be used as an ex post facto indicator of the wind azimuth during the event. [We must, however, be careful about using the orientation of snapped or bent boles as evidence for the effect of wind because, as reported by Proulx and Greene, 2001, trees with asymmetrical crowns (typical of steep slopes and forest edges) will bend or snap in the direction of the center of gravity (i.e., downslope or toward the clearing) regardless of the prevailing wind—at least when the wind is modest, as in the 1998 event. That is, one should use only flat areas to show, indirectly, the prevailing wind.]

A second prediction is that, in a typical icing event (and the subsequent period before the ice melts) assuming gusts of $10\,m\,s^{-1}$ in the midcanopy of a leafless hardwood forest, breakage of a ramified branch about 3 m long would occur with an equivalent radial ice thickness (t) on the order of 0.015 m (from Figs. 6.5 and 6.6). In the absence of wind, the required radial

ice thickness is only marginally smaller. One of us (Jones) has noted that significant tree damage begins at about 0.005 m radial ice thickness, although most shoots are simply sagging near their apical ends in response to the added weight. Proulx and Greene (2001) showed that breakage beyond the "background level" of crown loss from other previous minor disturbances began to be noticeable in northern hardwood stands only at ice diameters d_{max} on the order of 0.015 m. Branches with defects (see below) will have even lower minimum icing levels for breakage. Indeed, Lemon (1961) argued that breakage of branches with defects typically becomes noticeable with an added ice diameter of 0.006 m, and very common among such branches with an ice diameter of 0.0125 m. The ice diameter measurements d_{max} used by Lemon (1961) and Proulx and Greene (2001) are at least twice and perhaps significantly greater than twice the equivalent radial ice thickness: $t \leq d_{\max}/2$. These authors' d_{max} values of 0.015, 0.006, and 0.0125 m are consistent with equivalent radial ice thicknesses less than 0.007, 0.003, and 0.006 m, respectively. Thus, these studies are very roughly consonant: significant damage begins at a t value of about 0.003–0.005 m, with large numbers of (especially) defective branches falling if t reaches about 0.006 or 0.007 m.

As for healthy branches, Proulx and Greene (2001) observed that about 50% of the branches were removed (permanent bending and snapping are included in this tally) with icing diameters on the order of 0.045 m. Lemon (1961) observed that damage to healthy branches and snapping of small trees became widespread when the added ice diameter exceeded about 0.024 m. This range (t less than roughly 0.012–0.022) includes our expectation for breakage of a ramified 3 m long branch at $t = 0.015$ m (Fig. 6.6).

A third (and very obvious) prediction is that hollowed branches and those with stress risers should be the first to break. As the proportion of the central portion of a branch rots (and thus effectively hollows it out), the bending stress increases. Hollowness by itself only slightly increases the stress if the hollow is centered (Kane et al., 2001); e.g., if half the diameter is rotted wood, the stress is only about 6% higher. Much more important are cracks and cavities in the wood near the outside of the shoot (due to frost, lightning, beetle galleries, pitch pockets at old injury sites) that amplify stress and lead to crack propagation and, thus, eventually breakage. Structural failure of branches or boles has often been linked to the degree of rot and thus, very generally, to tree age. Empirical evidence and anecdotes for enhanced breakage due to rot and stress risers are numerous (e.g., Seischab et al., 1993; Bruederle and Stearns, 1985; Rhoads et al., 2002). Additionally, the

resulting new wounds from breakage significantly weaken the individual tree and greatly increase the risk of insect and fungal attacks after the icing event (Campbell, 1937; Melancon and Lechowicz, 1987; Rebertus et al., 1997).

A fourth prediction involves higher vs lower branches. We set the height for evaluation of the wind speed at 50% of crown length for a 25 m tall forest, pointing out the steep gradient from the top to the bottom of the canopy. Given that branch length increases with increasing distance from the top of the canopy, the short branches are mainly in the upper crown and are subjected to greater drag during an ice storm and more added ice weight. Thus, we can make a simple prediction: upper branches are much more likely to be broken than lower branches because they experience greater wind speeds while ice remains on the branches (causing larger wind drag) and they intercept some of the freezing precipitation so less water is available to freeze on the lower branches. For our assumed relationship between diameter and length, the highest stress at the base of unramified branches was for branches about 0.2 m long. These short branches will also be ramified but with many fewer side shoots than our sample 2.76 m long branch. The probably greater radial ice thicknesses (along with the stress peak) for short branches should more than compensate for the greater ramification of the more lightly iced longer branches lower in the canopy. We can find no quantification of this in the literature, although it seems to us qualitatively to be correct on the basis of observations by two of us (Greene and Proulx) during modest icing levels. Note, however, how messy testing this prediction really will be: falling upper branches can add to the moment on lower branches with which they collide, thus decreasing the expected vertical gradient in branch loss.

A fifth prediction is that interspecific differences in wood density (characteristic breaking stress of the unseasoned wood) ought to be important. As mentioned above, the range of breaking stress values for unseasoned (green) wood is about threefold for most North American tree species. However, within a diverse eastern hardwood stand we might expect only a twofold range in breaking stress from 40 to 80 $MN\,m^{-2}$. A radial ice thickness of 0.03 m or more would cause inflexible unramified branches with a breaking stress of 40 $MN\,m^{-2}$ to fail. However, only at a radial ice thickness of 0.05 m or more would branches with a breaking stress of 80 $MN\,m^{-2}$ fail. This effect of species-specific breaking stress may be difficult to recognize in the field because of other factors that influence the ability of the tree species in that hardwood stand to withstand ice loads, including the variation in ramification and branch angle (branching architecture), differences in branch

flexibility, characteristic differences in the position of that species in the canopy (this is not a successional argument: on average, shade-intolerant species will place their crowns higher in the canopy layer than will shade-tolerant species because the former cannot be present in the lower canopy stratum), differences in the age of the various tree species (and thus time for the development of stress risers due to fungal rot or insect-induced injury or previous exposure to damaging storms). Further, falling branches breaking lower branches and variations in breaking stress in different parts of the stem and canopy of individual trees will, of course, make it even more difficult to quantify the effect of wood density.

Ice measurements in the field

The foregoing analysis is useful only if it can be tested with field data. Clearly, we need studies that relate the consequences of an icing event (e.g., branch loss, subsequent mortality) to the ice thickness. Previous attempts at measurement of ice thicknesses prior to melting have been based on a few estimates made on fallen branches at one or two sites, or on interpolation of meteorological station data (e.g., Proulx and Greene, 2001). While it is difficult to make field measurements, it can be done, and we turn to field problems here.

Given the typically short period of ice persistence, it is crucial that the investigator drive to the site as soon as it becomes clear that a major event is occurring nearby. Some roads are usually closed because of fallen branches, boles, and power lines, but often a 4-wheel-drive vehicle can get around these obstacles.

Having arrived at a site of interest, one measures the ice on standing and fallen branches. The ice-covered branches are readily cut with a saw, and the mean radial ice thickness for a branch segment can be calculated (solving Eq. 6.3 for t) given the measured masses (ice plus wood minus wood alone), branch length, and branch diameter. The ice-covered branch samples are stored in zipper-lock plastic bags in a cooler and processed at the end of the day. The cooler keeps the ice at least partially frozen until the end of the day, and the sealed plastic bags (double bags, preferably) retain the melted water for that sample. (The goal at the end of the day is to find a place to stay where the power is on so that the samples collected that day can be processed!) The samples and bare branches are weighed on an electronic balance to 0.1 g, the branch length measured to 1 mm, and the diameters of the branch segment measured at a few locations to 0.1 mm, from which the

average diameter is determined for use in calculating the equivalent radial ice thickness. To provide a context for the ice thickness data, it is useful to record the GPS coordinates of the site (later one can determine elevation, slope angle, and other factors from digital elevation models), measure the wind speed and direction and temperature, record the height above ground and orientation of the sample, note the severity of damage, and photograph the site and samples.

The collection of ice data during and following a storm can be dangerous. The dangers include but are not limited to one-car and multi-car accidents, live power lines on the ground, falling trees and branches, slippery surfaces underfoot, and cold and wet conditions. (It becomes clearer why we have so little data on this disturbance type.)

In many cases, however, the investigator cannot reach the site until after the ice has melted. Using standard weather station data, rough stand-scale estimates of ice thickness can sometimes still be made. If the reporting station is near the site and at a similar altitude, then one can use the hourly measurements of the amount of freezing rain in the precipitation gage. To calculate the radial ice equivalent (t) using Eq. (6.3), the mean wind speed at the reporting station can be used, although this must be corrected for canopy position (e.g., the protocol in Greene and Johnson, 1996). However, if the site of interest is at a different altitude from the reporting station (e.g., a mountain slope vs an airport in the valley bottom) or some distance away, then the icing thickness cannot be reliably estimated; we are dealing with a wedge of cold air lying at an angle under warm air so, even if the temperatures at both the site and the station are below freezing, the type of precipitation will depend on the thickness of the wedge of cold air at each location. If the cold air layer is too thick or the warm air layer above it is thin, the precipitation will be ice pellets rather than freezing rain. Where there is no upper warm air layer, the precipitation will be snow. Furthermore, the amount of precipitation and the wind speed may differ significantly between the station and the site, both of which control the amount of ice that can accrete.

A final issue is whether we can experimentally test loading equations or the relationship between ice accumulation and branch diameter in the field. Lanctot et al. (1960) sprayed water on horizontal cylinders to simulate freezing rain; however, this experiment was done in the absence of wind to obtain even exposure of the cylinders to the spray. While it would be interesting to use a spray rig to create artificial freezing rain on tree branches, care must be taken in simulating natural icing conditions with appropriate drop sizes, precipitation rates, air temperatures, and wind

speeds. Furthermore, the drops must be created far enough above the branch that they have time to supercool before impact. In recent years research groups in Canada and the United States have initiated independent efforts to create artificial freezing rain (Nock et al., 2013, 2016; Rustad and Campbell, 2012; Fahey et al., 2020). We elaborate on these recent developments following the section below.

A review of the literature on tree damage due to icing events

Proulx and Greene (2001) argued that the *severity* of the damage will be primarily controlled by ice thickness while the *type* of damage would be controlled by the size of the tree. By contrast, other authors (e.g., Lemon, 1961; Bruederle and Stearns, 1985; Cannell and Morgan, 1989; Hauer et al., 1993; Seischab et al., 1993; Sampson and Wurtz, 1994) have claimed non-trivial roles for species-specific characteristics, such as branching architecture and wood density, and spatial effects, such as proximity to an edge or slope angle.

Types of damage in relation to tree size

Broadly, there are three types of significant ice-induced damage to trees: permanent bole bending, bole failure (snapping), and major branch loss. The biomechanical analysis above was for the latter category but is also applicable to bole failure. Permanent bending ranges from minor deviations from the perpendicular position to the extreme case in which a tree bole is arched over until its crown is resting on the ground. The extreme case is of more interest to us because stems bent to the ground for a long period almost never, it would appear, regain their place in the canopy (Carvell et al., 1957; Lemon, 1961), although we can find no quantitative study of this. Tree injury by stem bending ranges from relatively inconsequential (temporary) to catastrophic (permanent). Smaller-diameter canopy individuals are more likely to bend permanently in response to ice loading (Downs, 1938; Spaulding and Bratton, 1946; Shepard, 1975; Sisinni et al., 1995). One study found that for three northern hardwood species, permanent bending was almost entirely limited to stems with diameter at breast height (dbh) less than 0.18 m (Proulx and Greene, 2001) and was the predominant mode of failure for stems with dbh less than about 0.1 m. Also, these authors found that dbh was a more crucial determinant of bending than was species identity,

accounting for four times more of the explained variation. This is not to deny that some species with characteristically fine branches (e.g., birch) tend to bend more than others (Lemon, 1961) but merely to relegate species differences to the status of minor factors.

Many authors have speculated that an individual stem's position in the canopy influences its susceptibility to icing injury (e.g., Bruederle and Stearns, 1985), assuming that understory stems are less susceptible to damage (Downs, 1938; Boerner et al., 1988; Seischab et al., 1993; Hauer et al., 1994) because most of the ice is intercepted by the top of the canopy. While this ought to be true (as we argued above), we point out that there is no convincing evidence that it is indeed correct. Perhaps a comparison of the breakage among boles and branches in the subcanopy of an intact forest vs equal-sized stems in adjacent small forest gaps would be the best way to tackle this issue; differences in wind speed and ice deposition would be minimized while the contrast in interception would be strong.

Snapping refers to trees whose trunks have been completely severed or remain attached by only a small amount of bark or wood. Proulx and Greene (2001) found that boles of intermediate diameter (approximately 0.1–0.2 m dbh) were most likely to fail. We should note that unlike the damage during catastrophic wind events, uprooting is not common for storms in the higher latitudes (e.g., southern Canada and the northern tier of states in the United States) that occur in mid to late winter because the ground is, except in rare instances, frozen at the time of the icing event. Further south, however, and in that subset of major icing events occurring near the beginning of the winter season, uprooting during severe icing events can be common.

The bigger trees, whose basal diameters preclude bending or snapping, tend to suffer severe branch loss given high-magnitude ice loading (Hauer et al., 1993; Sisinni et al., 1995; Proulx and Greene, 2001; Rhoads et al., 2002). The intuitive explanation (from Proulx and Greene, 2001) for the foregoing size-related damage under a severe loading is as follows. Very small boles (<0.01 m dbh) sometimes bend dramatically but are sufficiently resilient that they bend back after the load is released. Boles with a dbh of 0.01–0.1 m will bend without snapping but often cannot bend back if the load has been maintained for too long a period. It is noteworthy that their small low-order branches do bend back after the ice melts (a qualitative observation by two of us (Greene and Proulx)) while the trunk remains strongly curved. Larger boles (0.1–0.2 m dbh) have high-order branches that bend without breaking, but the accumulated load is too great and the bole itself breaks. (Whether wind is crucial for snapping [and less important for

branch loss or permanent bending] has never been discussed in the literature.) Finally, the larger hardwood boles (>0.2 m dbh) have high-order branches, at a variety of angles but not departing too far from being parallel to the forest floor (the angle where weight will be most effective) that break, thus reducing the load on the bole. Older stands composed of such large trees tend to look, after a major icing event, like World War I battlefields, the individual boles standing with their appended large-diameter branch stubs, a meter or so in length, each revealing cream-colored wood.

Other factors influencing icing damage to trees

Aside from tree size, susceptibility to icing damage is influenced by other factors that are typically defined qualitatively: branching architecture, species, crown asymmetry, and position of the tree in the canopy (Lemon, 1961; Bruederle and Stearns, 1985; Cannell and Morgan, 1989; Seischab et al., 1993; Rebertus et al., 1997; Proulx and Greene, 2001).

Branching architecture

Strong horizontal branching and a large surface area associated with many fine branches increase exposed surface area and ought to increase susceptibility to icing injury (Lemon, 1961; Cannell and Morgan, 1989). Such assertions have been quite informal in the literature, but it might be useful to look at the extremes. Do conifers (ignoring *Larix*), possessing much larger amount of winter surface area (leaves), tend to experience more damage? The discussion is complicated by the fact that non-*Pinus* conifers such as *Tsuga* or *Abies* tend to have thin, short branches (increasingly short with height), while *Pinus* is more like hardwoods in possessing longer, thicker branches. A final complication is due to the lower wind speeds (at any height) within a stand rich in conifers: the same needles that gather ice will also reduce the ambient wind speed. (Our argument here is for the augmentation of ice by the wind rather than the drag it induces.) Amid this confounding of our intuition, the empirical literature provides no guidance—at least at first glance. While several studies of mixed stands have found needle-leaved trees more vulnerable to icing injury (Illick, 1916; Lemon, 1961; Whitney and Johnson, 1984; Bruederle and Stearns, 1985; Boerner et al., 1988; Warrillow and Mou, 1999; Smith, 2000), other research has claimed that conifer species are less susceptible to icing damage than hardwoods (Rogers, 1924; Carvell et al., 1957; Hauer et al., 1993; Amateis and Burkhart, 1996; Irland, 1998; Manion et al., 2001). Note, however, that if we remove *Pinus* from the analysis, the preponderance of the foregoing evidence is that non-*Pinus* conifers

are much less damaged than are hardwoods. Nonetheless, the reader is reminded that in none of these studies is there any surety that ambient icing precipitation and species identity are independent when the study area is sufficiently large to include significant differences in ice thickness. In mountains in particular, both species' abundance and ice thickness can change markedly across a few 100 m perpendicular to the contours.

Species identity

Lemon (1961) first proposed the idea that species-specific wood density or (a measure it is proportional to) breaking stress ought to be important determinants of the probability of damage or death. It is no coincidence that these two parameters, the most easily obtained quantitative measures of interest, have been discussed so much in the literature. Nonetheless, Lemon (1961) found no significant relationship between either measure and his qualitative damage categories. Since then, his conclusion that there was no relationship between wood strength and susceptibility to icing injury has been supported by others (Deuber, 1940; Carvell et al., 1957; Hauer et al., 1994), although Jones et al. (2001) suggested that greater wood strength may help protect against secondary damage inflicted by overstory stem failure or falling branches. To provide an example with a common species from eastern forests, three studies of three different icing events resulted in very different conclusions for red maple (*Acer rubrum* L.). On a relative scale in diverse forests, we find that it is one of the most resistant species (Whitney and Johnson, 1984), moderately susceptible (Seischab et al., 1993), or one of the least resistant (Siccama et al., 1976). Clearly, as we have stressed above, many other confounding factors can play a role. But it is disheartening to note that the only good generalization we can make from the voluminous ice damage literature is that non-*Pinus* conifers are damaged more than hardwoods.

Crown asymmetry (proximity to edge or slope angle)

It has been asserted that the smaller, more narrow, crowns of interior forest trees are less likely to be damaged than the wider crowns of edge trees (Hauer et al., 1993). Crown asymmetry at stand perimeters or large gap margins appears to predispose edge trees to bending damage and, of course, edge trees should experience higher wind speeds (and therefore greater ice deposition) on the nonwindward side of a clearing (Illick, 1916; Seischab et al., 1993; Hauer et al., 1994; Sampson and Wurtz, 1994). Similarly, crown asymmetry of trees located on slopes predisposes them to greater damage because of unbalanced ice loading (Bruederle and Stearns, 1985; Seischab

et al., 1993). Proulx and Greene (2001) found that edge trees on flat ground bent away from the hardwood forest irrespective of the prevailing wind or direction that the edge faced. Trees on slopes also bent downslope, regardless of the prevailing wind or azimuth. Nonetheless, Proulx and Greene (2001) found that edge trees were not significantly more likely to be in the heavily damaged category than interior trees when the ice load was extreme (1998: near the Quebec-New York border; modest ambient wind speeds) and with heavy damage including catastrophic branch loss and snapping as well as permanent bending. We should not exaggerate the increase in wind speed on nonwindward vs windward clearing edges in clearings (say, 200 m on a side). For such openings in forests or in agricultural terrain *in full leaf*, the wind has little time to accelerate across the clearing (<twofold) by the time it is within 1 tree height of the leeward edge (Greene and Johnson, 1996). Further, as the wind approaches within 1 tree height of the leeward edge, it decelerates by about 50%. (Unfortunately, we know of no comparable data for leafless forests, but the point is that the extra ice due to enhanced wind speeds on nonwindward edges will not be nearly as strong an effect as one might have initially supposed. If the wind at midcrown height in a leafless forest far from any edge is about 45% of the speed at some reference height, clearly the speed at a nonwindward clearing edge cannot be even twofold greater.)

Position of the tree in the canopy

In addition to direct damage (wind-augmented or not) by ice accumulation, understory trees are, at the same time, prone to injury resulting from indirect damage as snapped boles or branches fall from the canopy. Duguay et al. (2001) reported that only 22% of the shorter understory saplings avoided being pinned or crushed by falling branches at St. Hilaire, Quebec, during and after the 1998 ice storm. Likewise, one presumes (there are no empirical reports) that many of the lower branches on canopy trees are pruned by the additional load imposed by falling branches from higher in the crown.

The population consequences of major ice events

By definition, any disturbance has a direct effect on population dynamics because it represents the death of a reproductive mature tree. But, as was made clear by the gap dynamics studies of the 1970s and 1980s (Pickett and White, 1985), disturbances are also sources of "births" (broadly defined): postdisturbance asexual and sexual recruitment, as well

as release among the advance regeneration (e.g., Oliver and Stephens, 1977). While gap creation and the pulse of woody debris following severe events have numerous effects on animal communities (e.g., Faccio, 2003) and hydrological systems (Kraft et al., 2002), our concern here is with tree populations. Arched trees and snapped trees can be considered as deaths. Stems bent dramatically toward the ground never regain their original form (Rhoades, 1918; Carvell et al., 1957; Lemon, 1961), while snapped trees have lost their crowns completely. They may still be alive, resprouting vigorously from the root collar or, for a few species, from root suckers. But they will have to rebuild their trunks and crowns de novo.

For hardwood trees suffering major branch loss, Shortle and Smith (1998) suggested the following rules for predicting long-term impacts: (1) greater than 75% live crown loss: survival rate very poor, with surviving individuals likely to become heavily infected by fungi; (2) 50–75% crown loss: many trees likely to persist, with some loss of vigor owing to internal infections and growth suppression; and (3) less than 50% crown loss: high survivorship, with some individuals likely to experience only delayed growth. To a remarkable degree, this simple expectation has been borne out by permanent plot studies in sugar maple stands in southern Quebec (Boulet, 1998).

Immediately following a severe icing event, hardwoods with catastrophic branch loss produce small numbers of adventitious shoots along the trunk and major branches, but these shoots become less numerous and vigorous each year, the annual diameter increment narrowing. Meanwhile, fungal infection proceeds rapidly from each exposed branch stub, and insect predation becomes chronic (Campbell, 1937; Melancon and Lechowicz, 1987; Rebertus et al., 1997). An additional cause of stress is the immediate exposure of stems to the heat and drying effect of the sun (Spaulding and Bratton, 1946). Death for these trees is a slow process, occurring within 3–10 years after the event.

When viewed years later, ice-induced canopy gaps have a random, patchy distribution (Bruederle and Stearns, 1985) that may be influenced by local variation in precipitation and wind during the event. Unfortunately, there are no estimates of local variations in radial ice thickness at the scale of, say, 20–200 m. Within these gaps, as discussed below, advance regeneration and asexual recruits from "dead" canopy trees will, one presumes, seize the vacant space. Between the gaps, where canopy trees were heavily damaged but nonetheless recovered, shade-tolerant, surviving subcanopy stems

can be expected to show temporary release as in the classical gap dynamics argument (e.g., Frelich and Lorimer, 1991).

Following icing events, three methods of recruitment occur: release of advance regeneration and postdisturbance sexual and asexual regeneration. Perhaps the most crucial effect of a severe icing event on the subsequent regeneration is the dramatic increase of light at lower canopy levels and at the forest floor. Not surprisingly, it appears that the least damaged portion of the advance regeneration, the subcanopy stems not pinned by falling debris, dominate the race to form the new canopy (e.g., Whitney and Johnson, 1984). But this generalization is true, of course, only for stands with appreciable amounts of predisturbance subcanopy stems. Any disturbance regime, such as ice, wind, or insects, that leaves the lowest stratum of the canopy relatively unaffected will eventually have a low abundance of shade-intolerant species among both the canopy trees and the subcanopy stems: these disturbances promote regeneration by advance regeneration, which is necessarily moderately to very shade-tolerant. For example, in the old-growth hardwood forest of St. Hilaire (Quebec) following the December 1983 ice storm, there was a modest pulse of new recruits, but most of the regeneration was composed of advance regeneration, and these in turn supplied the individuals that are now the tallest members of the emerging new canopy (Fig. 6.7).

Why is there so little contribution made by the postdisturbance sexual recruitment? There is abundant light and, for the small-seeded species at

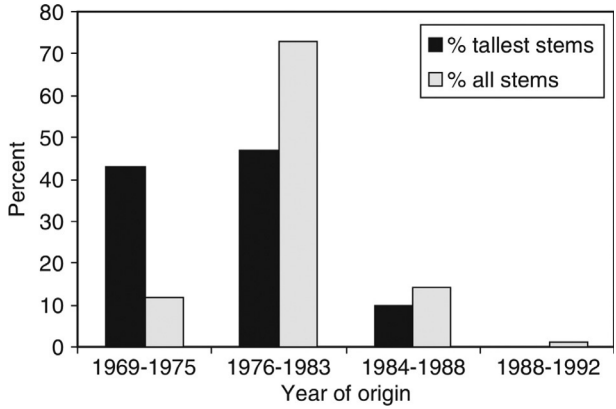

Fig. 6.7 Age structure of stems (almost entirely *Fagus grandifolium* and *Acer saccharum*) sampled in 1992 in a large gap created by the December 1983 ice storm at St. Hilaire, Quebec.

least, seedbeds are much improved by the dramatic reduction in leaf-fall that persists for the first few years. A permanent plot study at St. Hilaire, begun the year before the 1998 icing event and following a large seed crop (1996) by many species, has revealed that there has been almost no sexual reproduction since 1998. Fig. 6.8 shows eastern hemlock (*Tsuga canadensis* (L.) Carr.) as an example. The 2000 *Tsuga* cone crop (leading to the 2001 seedling cohort) was a mast event across southern Quebec except in the areas devastated by the 1998 ice storm. For equivalent tree size (basal area), it was visually estimated by using binoculars that the cone crop was eight times smaller for *Tsuga* at the badly damaged St. Hilaire site than at undamaged *Tsuga* stands located 100 km to the east in the foothills. This is hardly surprising—the living St. Hilaire *Tsuga* canopy trees had lost about half their crowns. Similarly, the 2000 cone crop for *Pinus strobus* L. (white pine) was six times smaller at St. Hilaire than the crop for equal-sized trees outside the ice storm area. Thus, a severely damaged tree with a reduced crown cannot produce large seed crops. The literature emphasis on "stress crops" (i.e., unusually large crops occurring in response to damage such as girdling or severe droughts) makes little sense to the present authors for severe icing events or any other natural disturbance.

Another way to regenerate following icing disturbance is asexually from basal sprouts or root suckers. Fig. 6.9 shows a permanent plot example for suckering in *Populus grandidentatum* Michx.; the results are similar to those for other *Populus* species following fire or clearcutting (Greene and Johnson, 1999). The sudden reduction of auxins transported from the crown

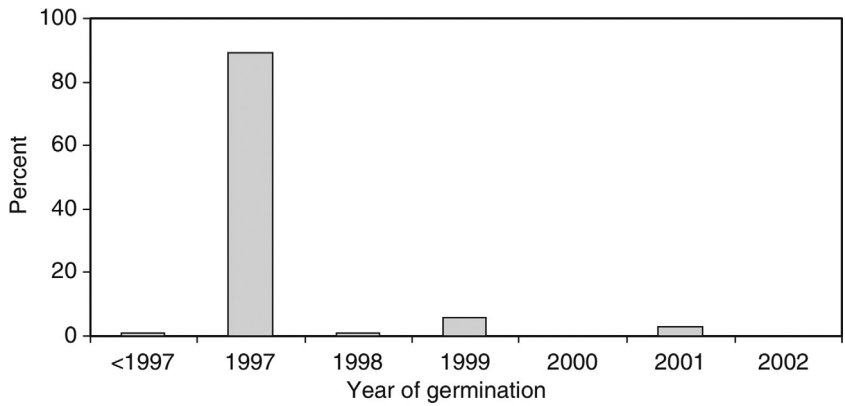

Fig. 6.8 Age structure of *Tsuga canadensis* derived from permanent plots in a stand devastated by the 1998 (January) ice storm at St. Hilaire, Quebec.

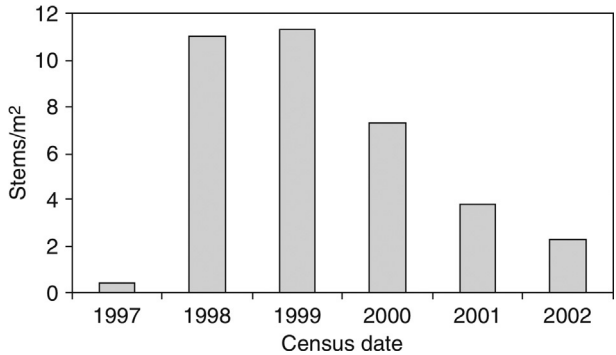

Fig. 6.9 Number of asexual stems of *Populus grandidentatum* in a permanent plot at St. Hilaire (Quebec) as effected by the January 1998 ice storm. "Births" were mainly in 1998; self-thinning began in 2000.

following the disturbance ends the dormancy of subaerial buds. The rapid proliferation of fast-growing asexual stems leads to a quick onset of self-thinning as these stems compete for both light and a shrinking starch reserve in the communal root system. Likewise, many hardwood species such as yellow poplar (*Liriodendron tulipifera* L.) and red maple commonly regenerate well from basal sprouts (Whitney and Johnson, 1984) and then rapidly thin. Whether sprouts or suckers seize the opened canopy space will depend on whether taller nearby advance regeneration has survived. This competition with the surviving advance regeneration is especially important for shade-intolerant species such as *Populus*.

Whether icing events are important for tree population dynamics in a region depends on the mean recurrence interval for severe events relative to the mean recurrence interval for other types of disturbance. Because of the small bending stresses from wind drag over the range of likely gust speeds, severe ice storms can be quantified by the radial ice thickness alone. Given the 75% crown loss rule for mortality in hardwood species, Proulx and Greene (2001) showed that the probability of a canopy tree dying was about 0.1 for a maximum radial ice thickness (t_{max}) of 0.025 m, 0.25 for t_{max} of 0.03 m, and about half the trees in a stand should die when $t_{max} = 0.045$ m. (Note: these ice thicknesses are from the Hydro Quebec Passive Ice Meters from the measurement of the *maximum* iced diameter of 0.025-m-diameter horizontal dowels. The relationship between t_{max} and t depends on the shape of the ice accretion, with t_{max} often significantly greater than t.) In Quebec, near the Canada–United States border, we expect t to be about 0.025 m for a 50 year mean recurrence interval and about 0.028 for a 100 year mean recurrence interval (CSA, 2001).

Thus, we expect that icing events will be recurrent, devastating events in the maple- and beech-dominated forests that typify this region (Melancon and Lechowicz, 1987; Duguay et al., 2001; Proulx and Greene, 2001). For a canopy tree of some shade-tolerant species, much of its life (typically 150 years in total: references in Proulx and Greene, 2001) will have been spent in the understory where, as discussed above, it would have been relatively impervious to ice storm damage because of its small pliable stem. Released by the death of an overtopping tree, the residency of this shade-tolerant individual in the canopy stratum after a brief period of rapid height growth would be, one speculates, quite short because of subsequent icing events.

By contrast, to the north of this area in the eastern boreal forest, the 50-year mean recurrence interval radial ice thickness is much smaller (CSA, 2001). This region has a fire regime with a mean recurrence interval (at least for the last few centuries) of about 150 years. Thus, given a cumulative exponential distribution with constant hazard of burning, the probability of a stand burning within 50 years is 0.28. In short, icing events ought to be a minor player in the eastern boreal forest because, simply, other events (fire and, for conifer species, spruce budworm epidemics) are far more common. As for the western North American boreal forest, the radial ice thickness for a 50-year mean recurrence interval is even smaller than in the east, while the mean fire interval is shorter (i.e., ice events are far too rare to have a major role in shaping the canopy tree mortality regime).

Experimental icing

Human-induced climate change is alteration of the frequency and severity of extreme climate events (IPCC, 2007). Future projections for the northeastern United States and eastern Canada suggest that there will be greater frequency and severity of ice storms in the future (Cheng et al., 2007, 2011; Hayhoe et al., 2007). However, our understanding of the effects of ice storms on forests has been limited by a number of challenges: first, ice storms leading to significant ice loading generally occur infrequently (Fig. 6.1), and second, they tend to have highly variable local and regional impacts. Experimental icing evolved in response to these challenges and is increasingly being employed to develop both: (i) a better understanding of within-crown ice distribution and (ii) a better understanding of relationships between the severity and frequency of ice storms and icing impacts on canopy structure and forest ecosystem function (e.g., Rustad and Campbell, 2012).

General considerations

Implementation of an experimental approach to studying the effects of ice loads at the tree level or stand level requires careful consideration of a method for simulating freezing rain. To briefly recap, ice storms form when moisture-laden warmer air overrides a layer of colder air at ground level. Rain drops falling from the warmer upper layer pass through the cold layer and cool. Drops may supercool (although supercooling is not a precondition for freezing rain) as they pass through the cold layer and freeze when striking sufficiently cold objects such as tree branches at ground level.

Important considerations when attempting to simulate ice storms include: the prevalence of subzero temperatures, proximity to source of water, and source water temperature. Based on air temperatures and source water temperatures, a water distribution system needs to be designed. It is important for the water distribution system to be able to move the water to spraying points without freezing, and for the sprinkling system to be able to distribute the water into the canopy. A sprinkling system will have a characteristic drop size distribution that can be measured (Nock et al., 2013), which will influence the likelihood of drops freezing on contact with branches, as opposed to remaining liquid and flowing or forming icicles. At one extreme, large rain drops will not freeze on contact and will result in flow along the branches and formation of icicles. At the other extreme, very fine drops tend to lead to entrapment of air during ice formation, resulting in a white colored ice that is not characteristic of freezing rain storms. Related to the drop size distribution is the rate of flow of water, which, if too low, can lead to freezing of the whole system and cessation of work for the day. Previous experiments have been successful at air temperatures from −14 to −9 °C utilizing municipal water and at −15 to −6 °C utilizing stream water (details in Nock et al., 2016; Rustad and Campbell, 2012).

To describe the magnitude of the experimental icing treatment, ice and water measurements are important. One logical choice is to utilize cylindrical dowels, which are utilized in many places to monitor ice loads (Nock et al., 2013). Total precipitation can be measured using buckets (Rustad and Campbell, 2012). Measuring resulting ice loads in the canopy is challenging but can be done on ice remaining on fallen broken branches, by accessing the canopy with scaffolding or a lift, or remotely via terrestrial laser scanning. Measurements of changes in canopy structure include quantification of canopy openness at the stand level using optical instruments, physical sampling of broken coarse and woody branches, as well as use of modern terrestrial laser scanning to capture pre-ice storm condition and post-ice storm changes to tree and canopy structure.

Tree level experiments

As noted above, despite the long-standing interest in ice storms the process of ice accretion and thus ice loading on branches remains poorly understood. In order to better understand the loading of branches and their biomechanical limits, one must first determine how ice accretes on branches; for example, is the radial ice thickness dependent or independent of diameter. This will determine if the load is calculated as a uniformly distributed load (independent) that does not vary along the branch or as load that varies with branch length (dependent). Such an understanding is a critical step for understanding variation in damage related to species identity and/or position in the canopy and for understanding how branch pruning in urban areas will influence crown ice loading and breakage. Earlier we noted upper branches intercept some of the freezing precipitation so less water is available to freeze on the lower branches. Similarly, within a crown, there is likely a bias toward the interception of precipitation at branch tips, resulting in greater accumulation and in turn leading to a positive feedback. This prediction was clearly borne out in experimental icing conducted by Nock et al. (2013). Comparing ice accretion on upper and lower branches on a Norway maple (Fig. 6.10) after 2.5 h of icing and after 6.5 h of icing, results for upper and lower (radial ice accretion 7 mm) were similar at 2.5 h, but by 6.5 h strongly differed (30 mm vs 12 mm; Nock et al., 2013). In addition, ice accretion varied along branches, declining toward the center of the crown as branch diameter increased.

By developing a process-based understanding of ice loading, future work may leverage progress in 3D modeling of tree crowns to develop simulations of how species with different branching patterns and crown forms intercept freezing rain. The idea that ice loading was heterogeneous first appears in Makkonen (2000), who suggested that ice loading varied by position within a crown, with lower branches generally receiving less ice due to branches above intercepting drops before they reach lower branches. Alternatively, one can describe this conceptual model as the following: the probability of a raindrop being intercepted by a canopy element can be expected to covary with the cumulative sum of branch area index above the element ($m^2\ m^{-2}$, analogous to leaf area index). This conceptual model of ice accretion (or attenuation) by tree crowns resembles the Beer–Lambert law (i.e., a negative exponential relationship), which is frequently applied in forests to describe the attenuation of light through the canopy (Sampson and Smith, 1993; Brown and Parker, 1994; Lieffers et al., 1999). Collection of terrestrial laser scanning data on 3D patterns of tree branching, in combination with

Fig. 6.10 Experimental icing in progress in February 2011 in Montréal, Québec, Canada. At center is a Norway maple that is 9 m tall with an approximate crown diameter of 5 m. Also visible are wooden dowels for measuring R_{eq} placed just beyond the drip line of the crown as well as underneath the crown.

experimental icing, allows for testing of this conceptual model. Nock et al. (2016) developed a quantitative model called IceCube to test the validity of this conceptual model of ice accretion, based on voxel-based description of freezing rain attenuation by canopies. Assuming for simplicity that rain falls primarily from the zenith, IceCube basically sums for a point on a target branch the number of voxels of the sample tree that are found within an inverted cone above the point. This sum was referred to as a sheltering factor. Measured ice accretion for the branches sampled was strongly related to variation in the sheltering factor. Because field experiments are challenging, the possibility of reproducing the observed patterns from IceCube was tested using a simulation model. The simulation model, IceTree, is adapted from models of canopy-light interactions employing z-buffering (depth buffering), and is capable of tracking the attenuation of freezing rain passing through 3D virtual plant canopies. Results from the simulated experiment were in accordance with empirical results (Nock et al., 2016). For both ecologists and forest managers, predicting ice accumulation is only a stepping stone to understanding branch rupture. Taking this step will require the coupling of biomechanical models of branch rupture with models of ice

accumulation. Experimental icing can provide a means of validation of loading and rupture for individual branches when such models are developed (Fig. 6.11).

Ecosystem response to ice storm disturbance: The Hubbard Brook Ice Storm Experiment

We noted above the need for studies that relate the consequences of an icing event (e.g., branch loss, subsequent mortality) to the ice thickness. Experimental approaches have also allowed researchers to start to address research questions focusing on forest ecosystem response to ice storm disturbance. Highly variable local and regional impacts of natural icing events lead to difficulties in establishing cause and effect relationships between ice loading and multiple variables—e.g., stand structure, composition—that often vary at the same scale as icing thickness. In contrast, the ability to implement ice loading and vary ice storm frequency and intensity of the canopy in a relatively homogenous area provides researchers with a clearer understanding of the variables contributing to canopy damage. For example, variation in species composition and average tree diameter or height can be controlled for during plot selection (Fig. 6.12).

Fig. 6.11 Collection of branches broken off the study tree presented in Fig. 6.10.

Fig. 6.12 Canopy icing in progress at Hubbard Brook for the Hubbard Brook Icing Experiment. Treatment plots were targeted by spraying water over the 15–20 m tall forest canopy from below. The falling water froze on contact with branches at air temperatures ranging from −14 to −9 °C. *(Photo credit: Lindsey Rustad).*

The ability to choose the location for an event also provides unique opportunities to study how similar disturbances in the past and present may be resulting in different effects due to changes in aspects of ecosystem function associated with global change. Experimental studies also facilitate our ability to predict how future changes in ice storm disturbance may impact forest ecosystems. For example, Fahey et al. (2020) were able to identify an important threshold for canopy damage and determine from repeated experimental icing that the effects of consecutive ice storms are likely to have marginal, as opposed to additive or multiplicative, effects. In a related study within the experiment, impacts of the simulated ice storm on losses of reactive N were examined and compared to losses resulting from a natural event of similar magnitude that occurred in the area decades earlier (Weitzman et al., 2019). Surprisingly, how the forest responded to icing damage in the past was quite different to the response observed in the experiment, perhaps as a result of N oligotrophication that has occurred at the HBEF over the past 30 years, but also potentially due to the less extensive canopy damage resulting from treatment of experimental plots. Further studies are needed to clarify if ecosystem responses to disturbances, such as ice storms, may be changing due to aspects of global environmental change.

References

Abell, C.A., 1934. Influence of glaze storms upon hardwood forests in the southern Appalachians. J. Forest. 32, 35–37.
Amateis, R.L., Burkhart, H.E., 1996. Impact of heavy glaze in a loblolly pine spacing trial. South. J. Appl. For. 20, 151–155.
ASCE, 2017. Minimum Design Loads for Buildings and Other Structures, Standard 7. American Society of Civil Engineers, Washington, DC.
Belanger, R.P., Godbee, J.F., Anderson, R.L., Paul, J.T., 1996. Ice damage in thinned and nonthinned loblolly pine plantations infected with fusiform rust. South. J. Appl. For. 20, 136–140.
Bisshopp, K.E., Drucker, D.C., 1945. Large deflection of cantilever beams. Q. Appl. Math. 3, 272–275.
Boerner, R.E.J., Runge, S.D., Cho, D.-S., Kooser, J.G., 1988. Localized ice storm damage in an Appalachian plateau watershed. Am. Midl. Nat. 119, 199–208.
Boulet, B., 1998. Management of ice storm damaged stands. Ministère Des Ressources Naturelles, Charlesbourg, QC.
Brown, M.J., Parker, G.G., 1994. Canopy light transmittance in a chronosequence of mixed-species deciduous forests. Can. J. For. Res. 24, 1694–1703.
Bruederle, L.P., Stearns, F.W., 1985. Ice storm damage to a southern Wisconsin Mesic forest. B Torrey Bot. Club 112, 167–175.
Campbell, W.A., 1937. Decay hazard resulting from ice damage to northern hardwoods. J. Forest. 35, 1156–1158.
Canadian Standards Association (CSA), 2001. CSA Standard C22.3 No. 1-01 Overhead Systems. Canadian Standards Association, Toronto, ON.
Canham, C.D., Loucks, O.L., 1984. Catastrophic windthrow in the presettlement forest of Wisconsin. Ecology 65, 803–809.
Cannell, M.G.R., Morgan, J., 1989. Branch breakage under snow and ice loads. Tree Physiol. 5, 307–317.
Carvell, K.L., Tryon, E.H., True, R.P., 1957. Effects of glaze on the development of Appalachian hardwoods. J. Forest. 55, 130–132.
Cheng, C., Auld, H., Li, G., Klaassen, J., Li, Q., 2007. Possible impacts of climate change on freezing rain in south-Central Canada using downscaled future climate scenarios. Nat. Hazards Earth Syst. Sci. 7, 71–87. https://doi.org/10.5194/nhess-7-71-2007.
Cheng, C.S., Li, G., Auld, H., 2011. Possible impacts of climate change on freezing rain using downscaled future climate scenarios: updated for Eastern Canada. Atmosphere-Ocean 49 (1), 8–21.
Deuber, C.G., 1940. The glaze storm of 1940. Am. Forests 46, 210.
Downs, A.A., 1938. Glaze damage in the birch-beech-maple-hemlock type of Pennsylvania and New York. J. Forest. 36, 63–70.
Duguay, S.M., Arii, K., Hooper, M., Lechowicz, M.J., 2001. Ice storm damage and early recovery in an old-growth forest. Environ. Monit. Assess. 67, 97–108.
Dunne, T., Leopold, L., 1978. Water in Environmental Planning. W. H. Freeman and Co., New York.
Elfashny, K., Chouinard, L.E., Laflamme, J., 1996. Estimation of combined wind and ice loads on telecommunication towers in Québec. Phase 1: modeling of the ice and wind observations. In: Laflamme, J., Farzaneh, M. (Eds.), Seventh International Workshop on Atmospheric Icing of Structures: Proceedings. Université du Québec à Chicoutimi, Chicoutimi, QC, pp. 137–141.
Faccio, S.D., 2003. Effects of ice storm-created gaps in forest breeding bird communities in Central Vermont. Forest Ecol. Manag. 186, 133–145.

Fahey, R.T., Atkins, J.W., Campbell, J.L., Rustad, L.E., Duffy, M., Driscoll, C.T., Fahey, T.J., Schaberg, P.G., 2020. Effects of an experimental ice storm on forest canopy structure. Can. J. For. Res. 50, 136–145.

Frelich, L.E., Lorimer, C.G., 1991. Natural disturbance regimes in hemlock-hardwood forests of the upper Great Lakes region. Ecol. Monogr. 61, 159–162.

Goebel, C.J., Deitschman, G.H., 1967. Ice storm damage to planted conifers in Iowa. J. Forest. 65, 496–497.

Greene, D.F., Johnson, E.A., 1996. Wind dispersal of seeds from a forest into a clearing. Ecology 77, 595–609.

Greene, D.F., Johnson, E.A., 1999. Modeling the recruitment of *Populus tremuloides*, *Pinus banksiana*, and *Picea mariana* following fire in the mixedwood boreal forest of Central Saskatchewan. Can. J. For. Res. 29, 462–473.

Harshberger, J.W., 1904. The relation of ice storms to trees. Contrib. Bot. Lab. Univ. Pennsylvania 2, 345–349.

Hauer, R.J., Wang, W., Dawson, J.O., 1993. Ice storm damage to urban trees. J. Arboric. 19, 187–193.

Hauer, R.J., Hruska, M.C., Dawson, J.O., 1994. Trees and Ice Storms: The Development of Ice Storm-resistant Urban Tree Populations. Special Pub. 94-1, Department of Forestry, University of Illinois at Urbana-Champaign, Urbana, IL.

Hayhoe, K., Wake, C.P., Huntington, T.G., Luo, L., Schwartz, M.D., Sheffield, J., Wood, E., Anderson, B., Bradbury, J., DeGaetano, A., Troy, T.J., Wolfe, D., 2007. Past and future changes in climate and hydrological indicators in the US northeast. Clim. Dyn. 28, 381–407. https://doi.org/10.1007/s00382-006-0187-8.

Illick, J.S., 1916. A destructive snow and ice storm. Forest Leaves 15, 103–107.

IPCC, 2007. Climate change 2007: the physical science basis. In: Solomon, S., Qin, D., Manning, M., Chen, Z., Marquis, M., Averyt, K.B., Tignor, M., Miller, H.L. (Eds.), Contribution of Working Group I to the Fourth Assessment Report of the Intergovernmental Panel on Climate Change. Cambridge University Press, New York.

Irland, L.C., 1998. Ice storm 1998 and the forests of the northeast: a preliminary assessment. J. Forest. 96, 32–40.

Jones, K.F., 1998. A simple model for freezing rain loads. Atmos. Res. 46, 87–97.

Jones, K.F., 1999. Ice storms, trees and power lines. In: Zufelt, J.E. (Ed.), Cold Regions Engineering: Putting Research into Practice: Proceedings of the Tenth International Conference. American Society of Civil Engineers, Reston, VA, pp. 757–767.

Jones, J., Pither, J., DeBruyn, R.D., Robertson, R.J., 2001. Modeling ice storm damage to a mature, mixed-species hardwood forest in eastern Ontario. Ecoscience 8, 513–521.

Jones, K.F., Thorkildson, R., Lott, N., 2002. The development of the map of extreme ice loads for ASCE Manual 74. In: Jackman, D.E. (Ed.), Electrical Transmission in a New Age: Proceedings of the Conference, September 9–September 12, 2002, Omaha, Nebraska. American Society of Civil Engineers, Reston, VA, pp. 9–31. Also published at ftp://ftp.ncdc.noaa.gov/pub/data/techrpts/tr200201/tr2002-01.pdf as *The Development of a U.S. Climatology of Extreme Ice Loads*. Technical Report 2002-01, U.S. Dept. of Commerce, NOAA/NESDIS, National Climate Data Center, Asheville, NC.

Kane, B., Ryan, D., Bloniarz, D.V., 2001. Comparing formulae that assess strength loss due to decay in trees. J Aboric. 27, 78–87.

Kienholz, R., 1941. Jack pine in Connecticut damaged by sleet storm. J. Forest. 39, 874–875.

Kraft, C.E., Schneider, R.L., Warren, D.R., 2002. Ice storm impacts on woody debris and debris dam formation in northeastern U.S. streams. Can. J. Fish. Aquat. Sci. 59, 1677–1684.

Lanctot, E.K., Peterson, E.L., House, H.E., Zobel, E.S., 1960. Ice build-up on conductors of different diameters. Trans. AIEE 46, 1610–1615.

Leister, A.T., Kemper, J.D., 1973. Analysis of stress distribution in the sapling tree trunk. J. Am. Soc. Hortic. Sci. 98, 164–170.
Lemon, P.C., 1961. Forest ecology of ice storms. B Torrey Bot. Club 88, 21–29.
Lieffers, V.J., Messier, C., Stadt, K.J., Gendron, F., Comeau, P.G., 1999. Predicting and managing light in the understory of boreal forests. Can. J. For. Res. 29, 796–811.
Lorimer, C.G., 1977. The presettlement forest and natural disturbance cycle of northeastern Maine. Ecology 58, 139–148.
Lorimer, C.D., Frelich, L.E., 1994. Natural disturbance regimes in old-growth northern hardwoods. J. Forest. 92, 33–38.
Makkonen, L., 2000. Models for the growth of rime, glaze, icicles and wet snow on structures. Philos. Trans. Roy. Soc. Lond. A Math. Phys. Eng. Sci. 358, 2913–2939.
Manion, P.D., Griffin, D.H., Rubin, B.J., 2001. Ice damage impacts on the health of the northern New York state forest. Forest. Chron. 77, 619–625.
McKay, G.A., Thompson, H.A., 1969. Estimating the hazard of ice accretion in Canada from climatological data. J. Appl. Meteorol. 8, 927–935.
Melancon, S., Lechowicz, M.J., 1987. Differences in the damage caused by glaze ice on codominant *Acer saccharum* and *Fagus grandifolia*. Can. J. Bot. 65, 1157–1159.
Nicholas, N.S., Zedaker, S.M., 1989. Ice damage in spruce-fir forests of the Black Mountains, North Carolina. Can. J. For. Res. 19, 1487–1491.
Niklas, K.J., 2000. Computing factors of safety against wind-induced tree stem damage. J. Exp. Bot. 51, 797–806.
Nock, C.A., Greene, D.F., Delagrange, S., Fournier, R., Messier, C., 2013. In situ quantification of experimental ice accretion on tree crowns using terrestrial laser scanning. PLoS One. 8(5), e64865. https://doi.org/10.1371/journal.pone.
Nock, C.A., Lecigne, B., Taugourdeau, O., Greene, D.F., Dauzat, J., Delagrange, S., Messier, C., 2016. Linking ice accretion and crown structure: towards a model of the effect of freezing rain on tree canopies. Ann. Bot. 117, 1163–1173.
Oliver, C.D., Stephens, E.P., 1977. Reconstruction of a mixed species forest in Central New England. Ecology 58, 562–572.
Pickett, S.T.A., White, P.S., 1985. The Ecology of Natural Disturbance and Patch Dynamics. Academic Press, Orlando, FL.
Proulx, O.J., Greene, D.F., 2001. The relationship between ice thickness and northern hardwood tree damage during ice storms. Can. J. For. Res. 31, 1758–1767.
Rebertus, A.J., Shifley, S.R., Richards, R.H., Roovers, L.M., 1997. Ice storm damage to an old-growth oak-hickory forest in Missouri. Am. Midl. Nat. 137, 48–61.
Rhoades, V., 1918. Ice storms in the southern Appalachians. Mon. Weather Rev. 46, 373–374.
Rhoads, A.G., Hamburg, S.P., Fahey, T.J., Siccama, T.G., Hane, E.N., Battles, J., Cogbill, C., Randall, J., Wilson, G., 2002. Effects of an intense ice storm on the structure of a northern hardwood forest. Can. J. For. Res. 32, 1763–1775.
Rogers, W.E., 1922. Ice storms and trees. Torreya 22, 61–63.
Rogers, W.E., 1923. Resistance of trees to ice-storm injury. Torreya 23, 95–99.
Rogers, W.E., 1924. Trees in a glaze storm. Tycos 14, 4–8.
Rustad, L.E., Campbell, J.L., 2012. A novel ice storm manipulation experiment in a northern hardwood forest. Can. J. For. Res. 42, 1810–1818.
Sampson, D.A., Smith, F.W., 1993. Influence of canopy architecture on light penetration in lodgepole pine (*Pinus contorta var. latifolia*) forests. Agric. Forest. Meteorol. 64, 63–79.
Sampson, G.R., Wurtz, T.L., 1994. Record interior Alaska snowfall effect on tree breakage. North. J. Appl. For. 11, 138–140.
Sanders, K.J., Barjenbruch, B.L., 2016. Analysis of ice-to-liquid ratios during freezing rain and the development of an ice accumulation model. Weather Forecast. 31, 1041–1060.

Schaub, W.R., 1996. Methods to estimate ice accumulations on surface structures. In: Laflamme, J., Farzaneh, M. (Eds.), Seventh International Workshop on Atmospheric Icing of Structures: Proceedings. Université du Québec à Chicoutimi, Chicoutimi, QC, pp. 183–188.

Seischab, F.K., Bernard, J.M., Eberle, M.D., 1993. Glaze storm damage to western New York forest communities. B Torrey Bot. Club 120, 64–72.

Shepard, R.K., 1975. Ice storm damage to loblolly pine in northern Louisiana. J. Forest. 73, 420–423.

Shortle, W. C., and Smith, K. T. (1998). Ice Storm 1998. Northeastern Forest Experiment Station Information Sheet # 1, March 3. USDA Forest Service, Durham, NH.

Siccama, T.G., Weir, G., Wallace, K., 1976. Ice damage in a mixed hardwood forest in Connecticut in relation to *Vitis* infestation. B Torrey Bot. Club 103, 180–183.

Sisinni, S.M., Zipperer, W.C., Pleninger, A.C., 1995. Impacts from a major ice storm: street-tree damage in Rochester, New York. J. Arboric. 21, 156–167.

Smith, W.H., 2000. Ice and forest health. North. J. Appl. For. 17, 16–19.

Spaulding, P., Bratton, A.W., 1946. Decay following glaze storm damage in woodlands of Central New York. J. Forest. 44, 515–519.

Von Schrenk, H., 1900. A severe sleet-storm. Trans. Acad. Sci. St. Louis 10, 143–160.

Warrillow, M., Mou, P., 1999. Ice storm damage to forest tree species in the ridge and valley region of southwestern Virginia. J. Torrey Bot. Soc. 126, 147–158.

Weitzman, J.N., Groffman, P.M., Campbell, J.L., Driscoll, C.T., Fahey, R.T., Fahey, T.J., Schaberg, P.G., Rustad, L.E., 2019. Ecosystem nitrogen response to a simulated ice storm in a northern hardwood forest. Ecosystems. https://doi.org/10.1007/s10021-019-00463-w.

Whitney, H.E., Johnson, W.C., 1984. Ice storms and forest succession in southern Virginia. B Torrey Bot. Club 111, 429–437.

Yorks, T.E., Adams, K.B., 2003. Restoration cutting as a management tool for regenerating *Pinus banksiana* after ice storm damage. Forest Ecol. Manag. 177, 85–94.